Available online at www.sciencedirect.com
SCIENCE DIRECT
Catalysis Today 111 (2006) 182–187
CATALYSIS TODAY
www.elsevier.com/locate/cattod

Size reduction of PtRu catalyst particle deposited on carbon support by addition of non-metallic elements

Hideo Daimon *, Yukiko Kurobe

Development and Technology Division, Hitachi Maxell Limited, 6-20-1 Kinunodai, Yawara-mura, Tsukuba-gun, Ibaraki 300-2496, Japan

Available online 15 December 2005

Abstract

Addition of non-metallic elements such as N, P and S was examined to reduce the catalyst particle size of PtRu deposited on a carbon support and to improve the catalytic performance. It was found that the addition of N, P and S reduced the size of PtRu catalyst particle and that P was the most effective additive on the size reduction. A well dispersed PtRu catalyst particle 2 nm in size was obtained by the addition of P. The maximum power density was observed to be 64 mW/cm^2 in a passive state of direct methanol fuel cell (DMFC) at room temperature by using the PtRuP anode catalyst. The PtRuP catalyst retained the size independently with surface area of the carbon support. This made it possible to use a carbon support with low surface area (lower porosity), resulting in better accessibility by molecules on the noble metal particles which were deposited prior to the external surface in compared to the micropore walls. The maximum power density was improved from 44 to 64 mW/cm^2 by using a less porous carbon support (140 m^2/g).

Keywords: Fuel cell; Size reduction; Addition of non-metallic elements; PtRuP catalyst

1. Introduction

For advances in fuel cells, catalytic activity and utilization efficiency of catalyst should be simultaneously improved. Reduction of the particle size of catalytic component is effective to improve its mass diffusion rate [1,2]. Generally, carbon supports with high specific surface areas are used to obtain fine Pt and PtRu catalyst particles [1–4]. However, micropores exist in the carbon supports and the fine catalyst particles may be buried in the micropores. The catalyst particles buried in the micropores may lose their opportunities to contact with solid polymer electrolyte and fuel, resulting in the loss of catalytic property. The fraction of buried catalyst should increase with higher specific surface area, which will deteriorate efficiency of the catalyst. Pt is an expensive material and its deposits in the world are very limited, but it is still the best catalyst for the fuel cell application. To realize the fuel cell application, improvement of the catalytic activity and minimization of the Pt requirement will be essential. Therefore, a new technology that can simultaneously improve the catalytic activity and utilization efficiency of the catalyst is strongly demanded.

Watanabe et al. synthesized 1.7 nm of well dispersed Pt catalyst particle by using a carbon support with specific surface area of 1250 m^2/g [2]. They stated that the area of wall of the micropores smaller than 2 nm in diameter was included in the Brunauer–Emmett–Teller (BET) surface area and the area mainly consisted of micropore walls on high surface area carbon supports, but the micropores should be inaccessible by molecules for both catalytic reaction and diffusion of oxygen. Efficiency of the Pt catalyst was electrochemically measured to be around 0.4 in their studies [5,6]. Therefore, it seems difficult to improve both activity and efficiency by enhancing the specific surface area of carbon supports resulting in the reduction of size of catalyst particle.

It has been reported that addition of a non-metallic element, P, drastically reduced the size of Fe single crystal in a magnetic alumite film [7]. In this report, a new method is proposed to reduce the size of PtRu catalyst particle. It is shown that the addition P reduces the size of PtRu catalyst particle and that reduced size is retained independently with the specific surface

* Corresponding author.
E-mail address: hideo-daimon@maxell.co.jp (H. Daimon).

0920-5861/$ – see front matter © 2005 Elsevier B.V. All rights reserved.
doi:10.1016/j.cattod.2005.10.023

area of the carbon support. It is demonstrated that the PtRuP catalyst is a promising candidate as both the catalytic activity and efficiency of catalyst are simultaneously improved.

2. Experimental

A PtRu catalyst was synthesized by a polyol process [8–11] using ethylene glycol as a reductant. 1.69 mmol of platinum (II) acetylacetonate ($Pt(acac)_2$), 1.69 mmol of ruthenium (III) acetylacetonate ($Ru(acac)_3$) and 0.5 g of carbon support were mixed in ethylene glycol and the solution was refluxed for 4 h at 473 K with mechanical stirring under nitrogen atmosphere. After refluxing, ethylene glycol was evaporated and the obtained PtRu catalyst was washed with ion exchanged water and then ethanol. The PtRu catalyst was dried under vacuum with a liquid nitrogen trap. Catalyst with PtRu loading of 50 wt.% was obtained by this procedure.

Addition of non-metallic elements such as B, N, Si, P and S to PtRu catalyst was conducted by co-feed of dimethylamine borane ($((CH_3)_2NHBH_3)$), sodium tetrahydroborate ($NaBH_4$), sodium nitrite ($NaNO_2$), sodium nitrate ($NaNO_3$), tetraethoxysilane ($Si(OC_2H_5)_4$), triphenylsilane ($((C_6H_5)_3SiH)$, sodium hypophosphite ($NaPH_2O_2$), disodium hydrogenphosphite (Na_2HPO_3), sodium dihydrogenphosphate (NaH_2PO_4), sodium sulfite (Na_2SO_3), sodium thiosulfate ($Na_2S_2O_3$) and sodium sulfate (Na_2SO_4) to the synthetic solution, respectively.

Morphology of the catalyst was observed by a transmission electron microscope (TEM, Hitachi, HF-2200). Noble metal particles deposited outside and inside of carbon support were observed by a scanning electron microscope (SEM, Hitachi, S-5200). Elemental analysis of the catalyst was carried out by using energy dispersive X-ray spectroscopy equipped with TEM (TEM-EDX, Noran Instruments), X-ray fluorescence spectroscopy (XRF, JEOL, JSX-3220ZS) and X-ray photoelectron spectroscopy (XPS, Perkin-Elmer, ESCA-5500MC). Crystallographic structure of the catalyst was analyzed by an X-ray diffractometer with Cu Kα radiation (XRD, Rigaku, RINT-1500).

Methanol oxidation activity was measured using linear sweep voltammetry with sweep rate of 50 mV/s. Working and counter electrodes were Au wires with diameter of 1 mm. Using Ag/AgCl reference electrode, potential–current curves were measured in solution containing 30 mg of supported the catalyst, 1.0 mol/l of sulfuric acid and 15 vol.% of methanol at 298 K in nitrogen atmosphere.

DMFC performance was evaluated under passive state at 298 K with a fuel of 15 wt.% methanol and ambient air. A mixture of the catalyst supported on carbon, ion exchanged water and Nafion solution (Aldrich, 5 and 10 wt.%) was coated on a Teflon sheet. After drying, the sheet was cut into circles with diameter of 18 mm and the circles were piled to get an electrode with 5 mg/cm^2 of catalyst for both anode and cathode. As a cathode catalyst, commercialized Pt catalyst (Taknaka Kikinzoku Kogyo K.K., TEC10E50E) was used. The anode and cathode electrodes were hot-pressed (433 K, 60 kgf/cm^2) on each side of solid polymer electrolyte (DuPont, Nafion 112 membrane, 50 μm in thickness) to make a membrane electrode assembly (MEA).

Table 1
Heat of mixing with Pt and Ru

Element	Heat of mixing with Pt (kJ/mol)	Heat of mixing with Ru (kJ/mol)
Pt	0	−1
Ru	−1	0
B	−13	−9
N	+103	+94
S	–	–
P	−26	−22
Si	−36	−21
Fe	−13	−5
Co	−7	−1
Ni	−5	0

Minus values indicate that the mixing is an exothermal reaction and the mixtures are energetically stabilized.

3. Results and discussion

At first in this study, a conventional PtRu catalyst was synthesized by a polyol process. TEM observation revealed that the size of PtRu catalyst particles was distributed from 2 to 10 nm and that its dispersion was heterogeneous. Maximum power density of DMFC using the PtRu anode catalyst was measured to be 38 mW/cm^2, which was far smaller than our target of 100 mW/cm^2. It has been reported that addition of P drastically reduced the size of acicular Fe single crystal in a magnetic alumite film [7]. In order to improve the catalytic activity of the PtRu, size reduction of PtRu catalyst particle by the addition of non-metallic elements was examined.

As additives of non-metallic elements, B, N, Si, P and S were selected. Table 1 summarizes heats of mixing of these elements with Pt and Ru [12]. In this table, heats of mixing in Pt–Pt and Ru–Ru are set to be zero and negative values indicate an exothermal reaction; the mixtures are energetically stabilized. Table 1 implies that metallic Pt–Pt and Ru–Ru bondings are replaced into Pt–X or Ru–X bondings by addition of most of non-metallic elements (X) which has a negative value in the heat of mixing. Since, the heat of mixing of Pt–Ru is slightly negative (−1 kJ/mol), a Pt–Ru bonding can be cut by the addition of non-metallic elements, B, P and Si. Therefore, it is expected that growth of PtRu is suppressed by the addition of these non-metallic elements. Table 2 shows effect of the additives on the size reduction of PtRu catalyst particles. The size was calculated by applying Scherrer's equation to (2 2 0)

Table 2
Effect of addition of non-metallic elements on size reduction of PtRu catalyst

Additive	Size of PtRu catalyst (nm)
Without	3.7
B	3.2
N	2.8
S	2.3
P	2.1
Si	3.3

Size of PtRu catalyst was calculated by applying Scherrer's equation to (2 2 0) diffraction peak of PtRu.

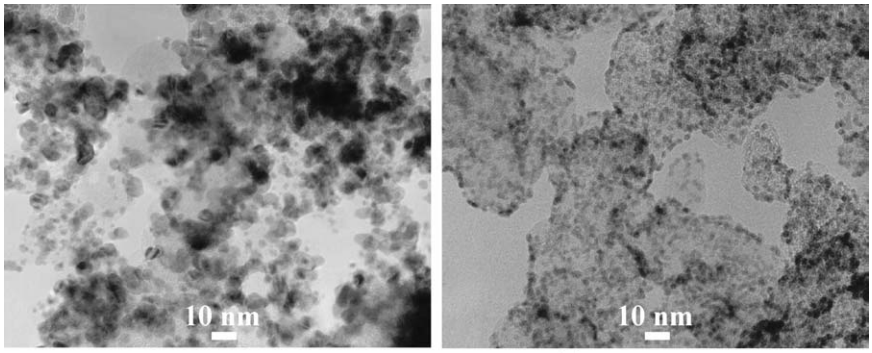

(A) $Pt_{60}Ru_{40}$ Catalyst (B) $Pt_{45}Ru_{44}P_{11}$ Catalyst

Fig. 1. TEM images of $Pt_{60}Ru_{40}$ and $Pt_{45}Ru_{44}P_{11}$ catalysts supported on Vulcan XC-72R. Specific surface area of Vulcan XC-72R:254 m^2/g.

diffraction peak of PtRu in XRD patterns. It was found that the addition of N, P and S reduced the size of PtRu catalyst particles; P was the most effective additive on the size reduction. Fig. 1 shows TEM images of $Pt_{60}Ru_{40}$ and $Pt_{45}Ru_{44}P_{11}$ catalysts supported on Vulcan XC-72R (Cabot Corp., Specific surface area: 254 m^2/g). The size of PtRu particles on the $Pt_{45}Ru_{44}P_{11}$ catalyst was reduced into 2 nm and dispersion of the catalyst component was improved compared with the $Pt_{60}Ru_{40}$ catalyst.

In Table 1, Fe, Co and Ni also have negative values in the heat of mixing with Pt and Ru and it is expected that the addition of these transition metals reduces the size of noble metal particle. Fig. 2 shows TEM image of a $Pt_{49}Fe_{51}$ catalyst supported on Ketjen Black EC (Lion, Specific surface area: 800 m^2/g). The size of metal particles on the $Pt_{49}Fe_{51}$ catalyst was reduced into 2–3 nm and the catalyst component was well dispersed. Watanabe et al. reported that PtFe, PtCo and PtNi alloyed anode catalysts showed an excellent CO tolerance [13]. From an industrial point of view, use of Fe, Co and Ni, instead of Ru, is preferred for cost reduction, because Fe, Co and Ni are less expensive than Ru. However, it seems not possible to use PtFe, PtCo and PtNi catalysts for the fuel cell. Since Fe, Co and Ni have negative values in a standard reduction potential of E^0 ($Fe^{2+} + 2e^- = Fe$ E^0−0.44 V, $Co^{2+} + 2e^- = Co$ E^0−0.28 V and $Ni^{2+} + 2e^- = Ni$ E^0−0.24 V, respectively [14]), these transition metals can easily be ionized in acidic circumstance. Nafion, DuPont's proton conductive membrane, is perfluoroalkylsulfonic acid and it is a super strong acid due to very high electronegativity of fluorine bonding with carbon which has been connected with a sulfonic acid group. The dissolved metallic ions can replace protons in the Nafion membrane and proton conductivity of Nafion membrane can be deteriorated. In a fact, the top of clear layer in the mixture of $Pt_{49}Fe_{51}$ catalyst, Nafion solution and ion exchanged water became yellow, indicating that the ionization of Fe occurred. On the other hand, non-metallic elements such as N, P and S have acid resistance and it should be possible to use these elements as additives.

Table 3 summarizes effectiveness of precursors for N, P and S on the size reduction of PtRu particles. Use of sodium nitrate ($NaNO_3$), sodium dihydrogenphosphate (NaH_2PO_4) and sodium sulfate (Na_2SO_4) as precursors for N, P and S was ineffective on the size reduction. Oxidation numbers of N, P and S atoms in these precursors reach their maximum values, +5, +5 and +6, respectively, implying chemical inactivity. This may be a reason for ineffectiveness of these precursors on the size reduction. On the other hand, the addition of precursors with lower oxidation state was effective on the size reduction. In these experiments, the addition of B and Si to PtRu catalyst

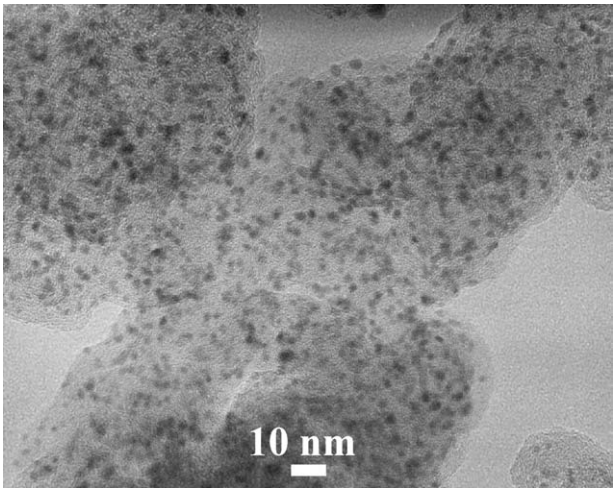

Fig. 2. TEM image of $Pt_{49}Fe_{51}$ catalyst supported on Ketjen Black EC.

Table 3
Effectiveness of precursors for N, P and S on size reduction of PtRu catalyst

Additive	Precursor	Oxidation number of element in precursor for source of additive	Size of PtRu (nm)
Without	–	–	3.7
N	$NaNO_2$	+3	2.8
	$NaNO_3$	+5	3.6
P	$NaPH_2O_2$	+1	2.1
	Na_2HPO_3	+3	2.2
	NaH_2PO_4	+5	3.6
S	$Na_2S_2O_3$	+2	2.3
	Na_2SO_3	+4	2.4
	Na_2SO_4	+6	3.7

Size of PtRu catalyst was calculated by applying Scherrer's equation to (2 2 0) diffraction peak of PtRu.

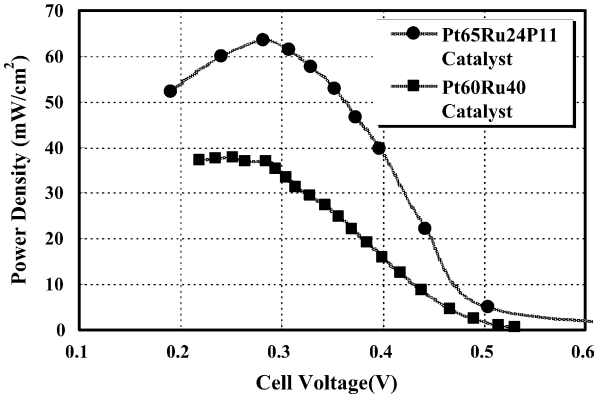

Fig. 3. Power density characteristics of DMFCs. Anode catalysts are $Pt_{60}Ru_{40}$ and $Pt_{65}Ru_{24}P_{11}$ supported on Vulcan XC-72R, respectively.

did not reduce the particle size well. These elements, however, have negative values in the heat of mixing with Pt and Ru as shown in Table 1. Therefore, the addition of B and Si should be effective on the size reduction by optimization of synthetic conditions such as pH in the synthetic solution and by selection of precursors for B and Si.

Optimization of the composition of PtRuP catalyst was carried out and it was found that $Pt_{65}Ru_{24}P_{11}$ catalyst was the most active for methanol oxidation. Polarization in methanol oxidation was suppressed by about 0.2 V at current density of 150 mA/cm^2 by using $Pt_{65}Ru_{24}P_{11}$ catalyst compared with $Pt_{60}Ru_{40}$ catalyst. Maximum power density in passive state of DMFC using $Pt_{65}Ru_{24}P_{11}$ anode catalyst was improved to 64 mW/cm^2 as shown in Fig. 3.

State of P in PtRuP catalyst was then analyzed. TEM-EDX analysis was carried out on center of the catalyst particle and on the surface of carbon support where there was no catalyst particle. The analyzed points are shown in scanning transmission electron microscopic (STEM) images in Fig. 4. As shown in Table 4, Pt, Ru and P were not detected on the surface of carbon support (analyzed points of C-1 and C-2). On the contrary, Pt, Ru and P were detected on the catalyst particles (analyzed points of PtRu-1 and PtRu-2). These results indicate that P and PtRu coexisted. Chemical state of P in PtRuP catalyst was analyzed by XPS and P_{2p} spectrum is shown in Fig. 5. There is no peak attributed to elemental state of P (129.8 eV) and there is a small peak attributed to metal phosphide (128.7 eV). There was a main peak around 133 eV of the binding energy, implying that most of P existed in oxidized

Table 4
Results of TEM-EDX analysis of PtRuP catalyst

Analyzed point	Composition (at.%)		
	Pt	Ru	P
C-1	0	0	0
C-2	0	0	0
PtRu-1	44	50	6
PtRu-2	39	54	7

TEM-EDX analysis was conducted on surface of carbon support (C-1, C-2) and on catalyst particles (PtRu-1, PtRu-2).

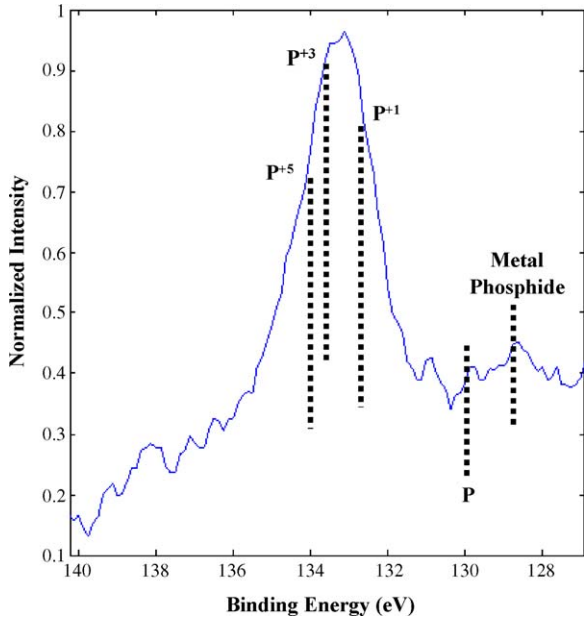

Fig. 5. P_{2p} XPS spectrum of $Pt_{48}Ru_{47}P_5$ catalyst.

state [15]. Content of P in the PtRuP catalyst was analyzed by XRF and XPS. Content of P analyzed by XPS was higher than that analyzed by XRF. Detection depth of XPS is much smaller than that of XRF, suggesting that P was enriched at the surface of PtRu catalyst particle. In a high resolution TEM image, clear lattice image was observed in each PtRuP catalyst particle, implying that PtRuP catalyst existed in nearly single crystal state. Change in lattice distance of (1 1 1) plane of the PtRu catalyst due to the addition of P was estimated by XRD. The lattice distance of (1 1 1) plane of 0.224 nm changed little by addition of P, suggesting little formation of interstitial

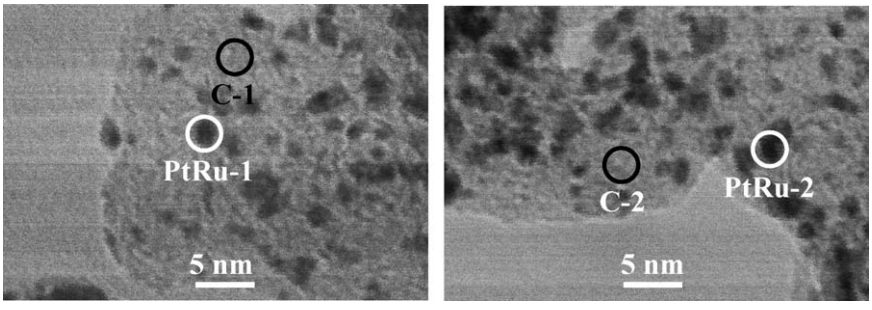

Fig. 4. STEM images of PtRuP catalyst in TEM-EDX analysis. White and black circles show analyzed points by TEM-EDX.

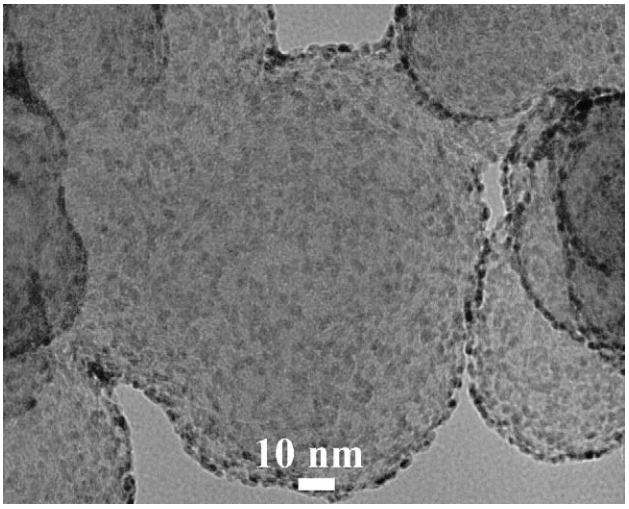

Fig. 6. TEM image of $Pt_{45}Ru_{44}P_{11}$ catalyst supported on Vulcan-P. Specific surface area of Vulcan-P:140 m^2/g.

compounds composed of PtP_x or RuP_x. Taking these analytical results into account, it is considered that P coexisted with PtRu particle and that most of P existed in oxidized state at surface of PtRu catalyst particle without forming interstitial compounds.

From Table 1, formation of Pt–P or Ru–P bonding (metal phosphide) is expected and these bondings are considered to reduce the size of PtRu catalyst particle. XPS analysis showed the existence of metal phosphide. However, the oxidized state of P was dominant in the PtRuP catalyst and XRD analysis showed there was little formation of PtP_x or RuP_x. In electroless plating of Ni, $NaPH_2O_2$ is known as a reductant; it is well known that P is incorporated into Ni and that Ni becomes amorphous by forming Ni phosphide. It was also reported that Fe phosphide was formed by electroplating with $NaPH_2O_2$ and that crystallographic continuity in Fe was disconnected [16]. Even though the amount of metal phosphide in PtRuP catalyst was small, the formation of the metal phosphide is considered to be a reason for the size reduction.

The other feature of PtRuP catalyst was retention of its size in 2 nm independently with specific surface area of carbon supports. Fig. 6 shows TEM image of a $Pt_{45}Ru_{44}P_{11}$ catalyst deposited on a carbon support having specific surface area of 140 m^2/g (Vulvan-P, Cabot Corp.). It can be seen that size of the catalyst particle was retained in 2 nm and that the catalyst component was well dispersed. Because the smaller surface area means less porosity, use of carbon with low surface area should improve the catalyst efficiency. Fig. 7 shows SEM and TEM images of a $Pt_{45}Ru_{44}P_{11}$ catalyst deposited on a porous carbon support of Ketjen Black EC with specific surface area of 800 m^2/g. In the SEM image, existence of catalyst particles (2 nm in size) was observed on the surface of carbon support. In the corresponding TEM image, observed number of the catalyst particles increased, implying that a large amount of the catalyst was buried in the micropores of the carbon support. Fig. 8 shows SEM and TEM images of the $Pt_{45}Ru_{44}P_{11}$catalyst deposited on less porous carbon support of Vulcan-P with specific surface area of 140 m^2/g. In the SEM image, it can be seen that the number of catalyst particles existing on the surface of carbon support is much larger than

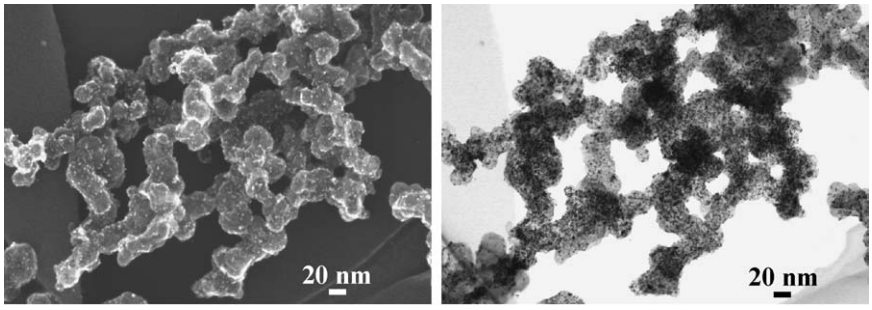

Fig. 7. SEM and TEM images of $Pt_{45}Ru_{44}P_{11}$ catalyst supported on Ketjen Black EC. Specific surface area of Ketjen Black EC:800 m^2/g.

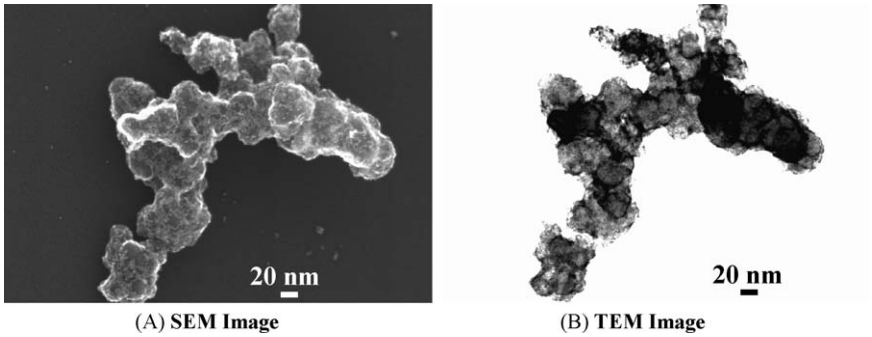

Fig. 8. SEM and TEM images of $Pt_{45}Ru_{44}P_{11}$ catalyst supported on Vulcan-P. Specific surface area of Vulcan-P:140 m^2/g.

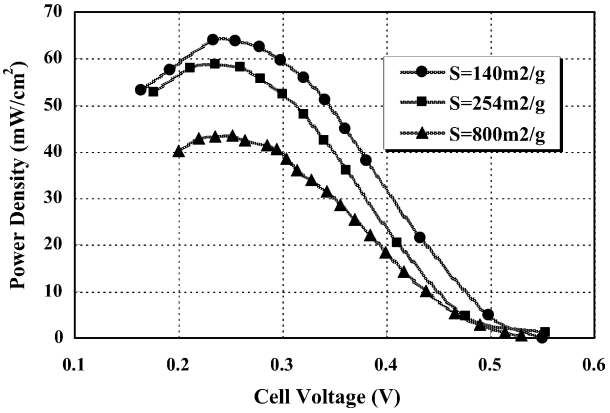

Fig. 9. Power density characteristics of DMFCs. Anode $Pt_{45}Ru_{44}P_{11}$ catalyst is deposited on carbon supports having specific surface area of 800, 254 and 140 m^2/g, respectively.

that on the carbon support with higher specific surface area (SEM image in Fig. 7).

Fig. 9 shows power density characteristics of DMFCs using the $Pt_{45}Ru_{44}P_{11}$ catalyst deposited on carbon supports with specific surface area of 800, 254 and 140 m^2/g. It is obvious that the power density of DMFCs was improved by using carbon supports with smaller specific surface area. This is attributed to improvement in efficiency of the catalyst caused by the increase in number of the catalyst existing on the surface of carbon supports. The PtRuP catalyst, which is deposited on less porous carbon supports and retains its size in 2 nm, is a promising candidate as both catalytic activity and efficiency of catalyst were simultaneously improved as above.

Acknowledgements

The authors are indebted to S. Suzuki, Dr. M. Sugimasa, Y. Arishima and Professor O. Kitakami of Tohoku University for their fruitful discussion. We give our thanks to M. Watanabe for TEM observation. We also wish to thank Dr. N. Ota and T. Taniguchi for their encouragement throughout this work.

References

[1] M. Watanabe, S. Saegusa, P. Stonehart, Chem. Lett. (1988) 1487.
[2] M. Watanabe, H. Sei, P. Stonehart, J. Electroanal. Chem. 261 (1989) 375.
[3] M. Uchida, Y. Aoyama, M. Tanabe, N. Yanagihara, N. Eda, A. Ohta, J. Electrochem. Soc. 142 (1995) 2572.
[4] M. Uchida, Y. Fukuoka, Y. Sugawara, N. Eda, A. Ohta, J. Electrochem. Soc. 143 (1996) 2245.
[5] M. Watabe, M. Tomikawa, S. Motoo, J. Electroanal. Chem. 182 (1985) 193.
[6] M. Watabe, M. Tomikawa, S. Motoo, J. Electroanal. Chem. 195 (1986) 81.
[7] H. Daimon, O. Kitakami, O. Inagoya, A. Sakemoto, Jpn. J. Appl. Phys. 30 (1991) 282.
[8] N. Toshima, M. Kuriyama, Y. Yamada, H. Hirai, Chem. Lett. (1981) 793.
[9] N. Toshima, Y. Wang, Langmuir 10 (1994) 4574.
[10] N. Toshima, Y. Wang, Adv. Matter. 6 (1994) 245.
[11] F. Fievet, J.P. Lagier, M. Figlarz, MRS Bull. 14 (1989) 29.
[12] F.R. de Boer, R. Boom, W.C.M. Mattens, A.R. Miedema, A.K. Niesse, Cohesion in Metals-Transition Metal Alloys, North-Holland, Amsterdam, 1999, p. 224.
[13] M. Watabe, Y. Zhu, H. Igarashi, H. Uchida, Electrochemistry 68 (2002) 244.
[14] F.A. Cotton, G. Wilkinson, Basic Inorganic Chemistry, John Wiley & Sons, New York, 1976, p. 378.
[15] C.D. Wagner, W.M. Riggs, L.E. Davis, J.F. Moulder, G.E. Muilenberg, Hand Book of X-ray Photoelectron Spectroscopy, Perkin-Elmer Corp., 1979,, p. 54.
[16] H. Daimon, O. Kitakami, H. Fujiwara, J. Mag. Soc. Jpn. 13 (Suppl. S1) (1989) 795.